JOURNAL OF MATERIALS SCIENCE 23 (1988) 570–576

Promotion of $ZnAl_2O_4$ formation by AlF_3

M. HASHIBA, Y. NURISHI, T. HIBINO
Department of Industrial Chemistry, Faculty of Engineering, Gifu University, Yanagido, Gifu-shi 501-11, Japan

Details of the formation of $ZnAl_2O_4$ in the presence of AlF_3 was studied for the purpose of elucidating the effect of fluoride anion on the reaction. In the $ZnO-AlF_3$ binary system, sublimation of AlF_3 and successive reaction of ZnO with AlF_3 vapour were the first route of $ZnAl_2O_4$ formation. $ZnAl_2O_4$ formation with AlF_3 was initiated at the $ZnO-AlF_3$ interface as well as that of the $ZnO-AlF_3$ binary system. This reaction was used to predict the formation of unstable zinc fluoride or zinc oxyfluoride. When the fluoride anions bound with zinc cations were transported to the surface of an Al_2O_3 particle, the intermediate phase was formed at the site. In addition, the vapour transport of AlF_3 to the $ZnO-Al_2O_3$ interface was expected to form an intermediate phase containing fluoride anions such as $Zn_aAl_bO_xF_y$ phase. The $ZnAl_2O_4$ formation was promoted by the material transport through the intermediate phase around Al_2O_3 particles.

1. Introduction

In a powdered solid state reaction, additions of additives promote the reaction [1, 2]. Halides, especially fluorides, are strong promoters [3–16]. Shimada *et al.* [17, 18] have studied the promotive effects of various fluorides on $MgAl_2O_4$ formation and reported the formation of AlF_3 during the reaction in the presence of LiF. We have found [19] that LiF forms an intermediate phase with LiF, ZnO and Al_2O_3 and the $ZnAl_2O_4$ formation is promoted by the migration of reactants through the intermediate phase. However, further dissolution of Al_2O_3 by the intermediate phase promoted the growth of a by-product ($LiAl_5O_8$). The $ZnAl_2O_4$ formation was interrupted by the formation of $LiAl_5O_8$. The role of LiF in the reaction must be a co-operative phenomenon of fluoride anion and lithium cation in the intermediate phase. However, complicated interaction in the intermediate phase has not been sufficiently analysed. This paper reports a study of the promotion of $ZnAl_2O_4$ formation by AlF_3. The promoting effect of the fluoride ion with no extra cations than those common to the reactants, was examined. Comparison of the results with LiF will differentiate between the effects of lithium cation from those of the fluoride ion.

2. Experimental procedure

2.1. Materials

Electrofused α-alumina of 60 μm average size was the source of α-Al_2O_3 particles, and spray-granulated α-Al_2O_3 of 40 μm average agglomerate size was the source of agglomerated Al_2O_3. Zinc oxide, 0.3 μm average size, was used. Aluminium fluoride was commercial extra-pure reagent and is composed of agglomerated particles.

2.2. Reaction mixtures

The following powder mixtures were prepared.

Sample I: mixtures of equimolar amounts of ZnO and AlF_3.

Sample II: mixtures of equimolar amounts of electrofused α-Al_2O_3 and AlF_3.

Sample III: 20 mol % AlF_3 was added to a mixture of equimolar amounts of coarse Al_2O_3 and ZnO.

Sample IV: 20 mol % AlF_3 was added to a mixture of equimolar amounts of agglomerates of fine Al_2O_3 and ZnO.

All samples were blended for 1 h in the dry state in a plastic bottle.

2.3. Compact formation and firing

The mixture was compacted in a 10 mm diameter steel die under a uniaxial pressure of 25 MPa. The powder compacts were fired in an electric furnace at preset temperatures for various durations. In order to avoid the effect of oxygen and water vapour on the reaction, the compacts were fired in an argon gas atmosphere. The argon gas used was dehydrated with silica gel, molecular sieves and P_2O_5, and then deoxygenated with titanium sponge heated at 800° C. For the purpose of water removal from the sample it was necessary to preheat it in the 300° C zone of the furnace for 1 h after evacuation using a rotary pump.

Thermogravimetric (TG) and differential thermal analysis (DTA) were carried out to examine the thermal behaviour of specimens on heating and cooling using the TG-DTA apparatus (Rigaku Denki Ltd).

2.4. Microstructural observation

Green and fired compacts were impregnated in epoxy resin and subjected to grinding and final polishing with 2 μm diamond paste. Polished samples were observed by optical microscopy in reflected light and also by scanning electron microscopy (SEM). The chemical composition of the phase in the microstructure was

0022–2461/88 $03.00 + .12

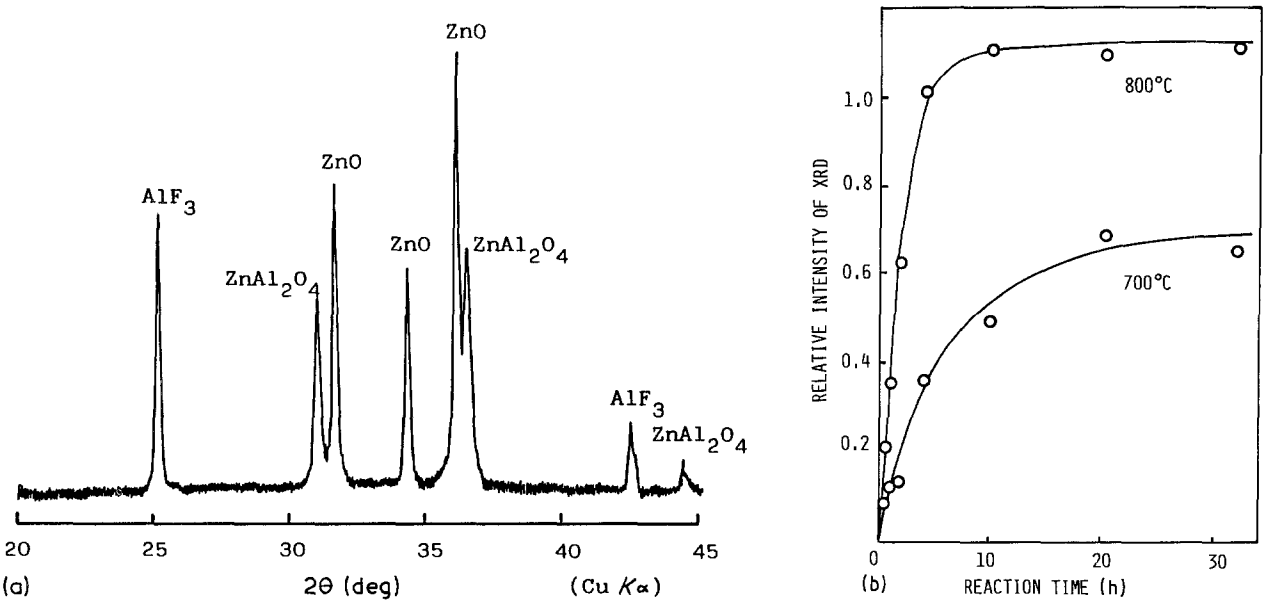

Figure 1 Reaction of ZnO and AlF_3. (a) X-ray diffraction pattern of sample I fired at 700° C for 10 h; (b) amount of $ZnAl_2O_4$ as a function of firing time.

analysed using an energy dispersive X-ray micro-analyser (EDX) (Horiba Ltd; model EMAX 8000S) attached to the SEM.

2.5. Detection of fluoride ions in the microstructure

We have proposed previously [20] to fix the fluoride ions as calcium fluoride and instead to follow the calcium ion signal on the polished surface using the EDX analyser which only has a weak sensitivity to fluoride ions [21]. The weak point of this method was that calcium ions cannot substitute for those cations which show a stronger affinity to fluoride ions than calcium ions, e.g. Al^{3+}. The method was improved by treatment with a solution containing thorium ions which have a much greater affinity to fluoride ions than calcium ions [22].

The polished surface of samples was digested in 0.15 mol l^{-1} thorium nitrate aqueous solution to fix the fluoride ions as thorium fluoride, followed by thoroughly washing with alcohol. After drying in an oven at 100° C for 1 h, the microstructure was observed and detected by the thorium instead of fluoride ion which coexists with aluminium or zinc in the microstructure by EDX analyser.

3. Results and discussion

3.1. Reactions in the ZnO–AlF_3 and Al_2O_3–AlF_3 systems

Fig. 1a shows the X-ray diffraction pattern of the ZnO–AlF_3 system fired at 700° C for 10 h. $ZnAl_2O_4$ is formed. But there are no crystalline products other than the reactants and $ZnAl_2O_4$. The amount of $ZnAl_2O_4$ gradually increased with firing time, as shown in Fig. 1b.

Fig. 2a shows the microstructure of the ZnO–AlF_3 system fired at 700° C for 10 h. The polished surface of the samples was treated with thorium nitrate solution to fix fluoride ion as thorium fluoride. Thorium is found in the ZnO phase by EDX analyser as shown in Fig. 2b, indicating that fluoride ions were transported from the AlF_3 phase to the ZnO phase. Fig. 2b also

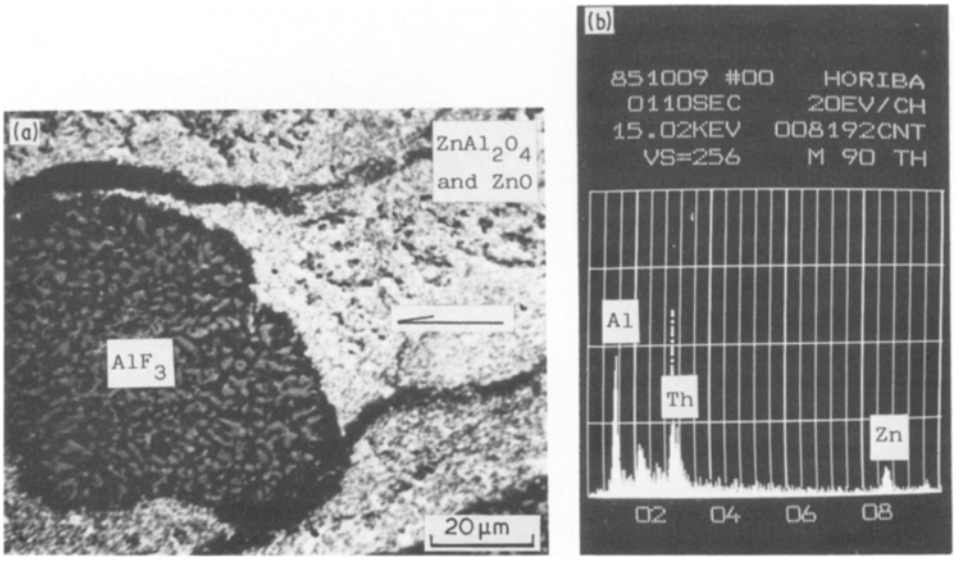

Figure 2 Microstructure of the ZnO–AlF_3 system. (a) SE image, (b) EDX analysis.

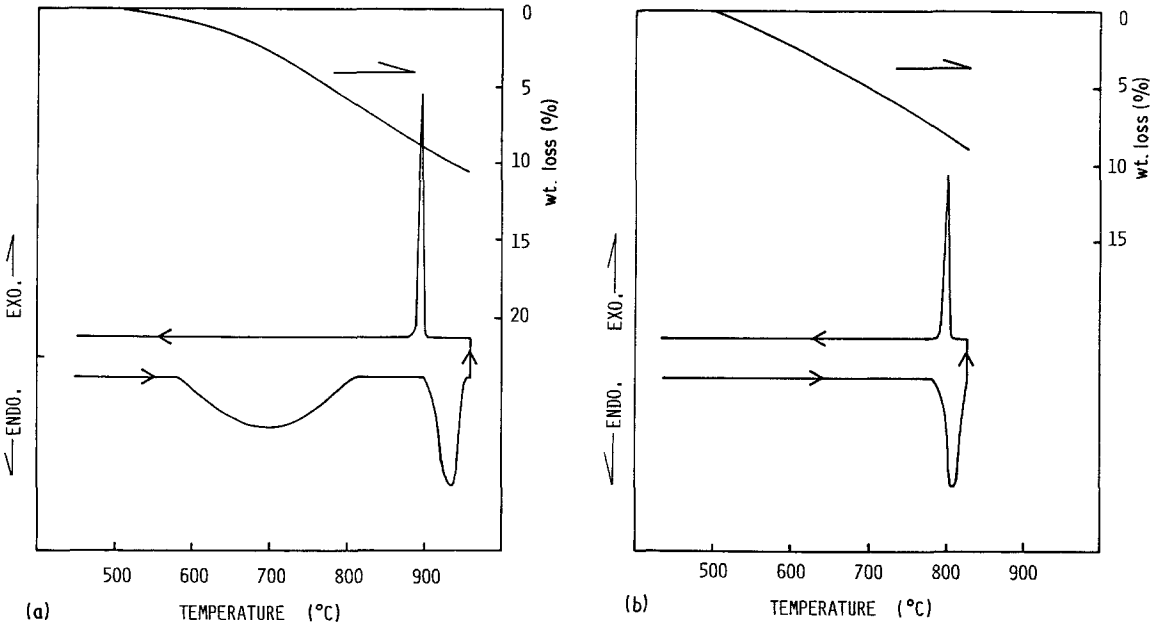

Figure 3 TG and DTA curves. (a) $ZnO-AlF_3$ system, (b) ZnF_2-AlF_3 system.

shows that EDX analysis of constituents, at the point marked in the ZnO phase in Fig. 2a, indicates the presence of aluminium in the ZnO phase. The amount of aluminium in the ZnO phase increased with firing time. On the other hand, zinc was not found in the AlF_3 phase. $ZnAl_2O_4$ would, therefore, have to form in the ZnO phase by reaction with transported AlF_3.

Fig. 3a shows TG and DTA curves for the $ZnO-AlF_3$ system. The weight reduction due to sublimation of AlF_3 and also the endothermic peak commence at 500° C. The TG curve for the ZnF_2-AlF_3 system in Fig. 3b shows that a weight reduction by sublimation of AlF_3 begins at 500° C in this system too. Interaction of oxygen ions of basic zinc oxide with acidic aluminium fluoride [23] must be the cause of the endothermic reaction observed in the $ZnO-AlF_3$ system.

Thermodynamic calculations [24–26] shown in Fig. 4, however, give a positive free energy change for the following solid–solid anion exchange reaction due to a strong affinity of aluminium ion for fluoride ions

$$3ZnO(s) + 2AlF_3(s) = Al_2O_3(s) + 3ZnF_2(s \text{ or } l)$$

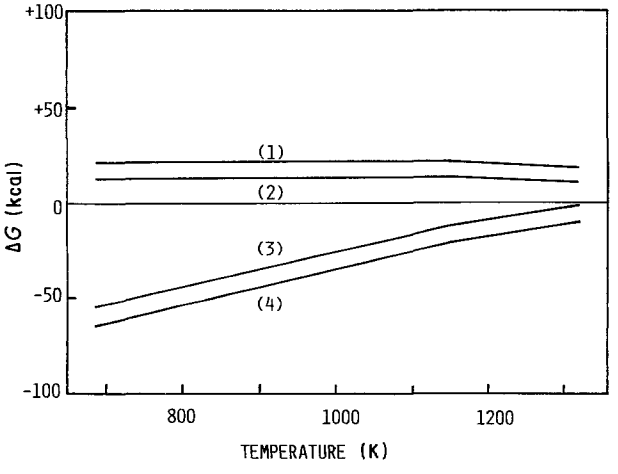

Figure 4 Free energy changes of reaction indicated as follows:
(1) $3ZnO(s) + 2AlF_3(s) = Al_2O_3(s) + 3ZnF_2(s \text{ or } l)$
(2) $4ZnO(s) + 2AlF_3(s) = ZnAl_2O_4(s) + 3ZnF_2(s \text{ or } l)$
(3) $3ZnO(s) + 2AlF_3(g) = Al_2O_3(s) + 3ZnF_2(s \text{ or } l)$
(4) $4ZnO(s) + 2AlF_3(g) = ZnAl_2O_4(s) + 3ZnF_2(s \text{ or } l)$.

Even if the reaction is accompanied by the formation of $ZnAl_2O_4$, as follows, the free energy change of the reaction is positive, as shown in Fig. 4

$$4ZnO(s) + 2AlF_3(s) = ZnAl_2O_4(s) + 3ZnF_2(s \text{ or } l)$$

The negative free energy change of formation of $ZnAl_2O_4$ from component oxides is not sufficient to compensate the positive free energy change of the anion exchange reaction between AlF_3 and ZnO.

Sublimation of aluminium fluoride [24, 25] could, however, help the free energy changes of the following reactions and then negative values for the reaction are obtained as shown in Fig. 4

$$3ZnO(s) + 2AlF_3(g) = Al_2O_3(s) + 3ZnF_2(s \text{ or } l)$$

$$4ZnO(s) + 2AlF_3(g) = ZnAl_2O_4(s) + 3ZnF_2(s \text{ or } l)$$

Sublimation of AlF_3 is thermodynamically necessary to form $ZnAl_2O_4$ in the $ZnO-AlF_3$ system with source of oxygen ions other than ZnO.

Fig. 5 shows the microstructure of the $Al_2O_3-AlF_3$

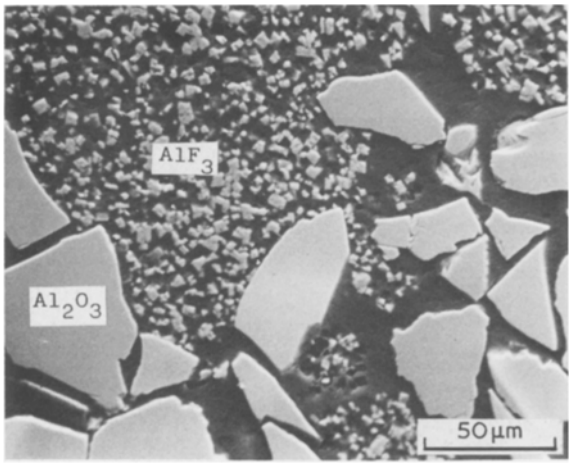

Figure 5 Microstructure of the $Al_2O_3-AlF_3$ system fired at 700° C for 10 h.

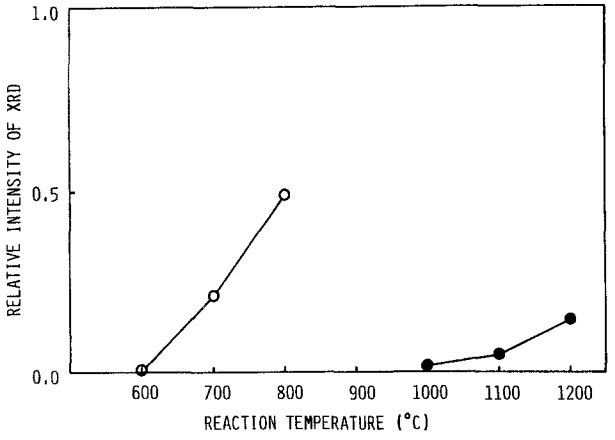

Figure 6 Formation of $ZnAl_2O_4$ from ZnO and coarse Al_2O_3 system with or without AlF_3, fired at various temperatures for 0.5 h. (○) ZnO–Al_2O_3–AlF_3 system, (●) ZnO–Al_2O_3 system.

system fired at 700° C for 10 h. No evidence of reaction at the interface between Al_2O_3 and AlF_3 is seen in the microstructure at this temperature.

3.2. Formation of $ZnAl_2O_4$ in the ZnO–coarse Al_2O_3–AlF_3 system

Relative peak heights of X-ray diffraction of $ZnAl_2O_4$ for the ZnO–coarse Al_2O_3–AlF_3 system and also for the ZnO–coarse Al_2O_3 system fired at various temperatures for 30 min, are plotted against the firing temperature in Fig. 6. $ZnAl_2O_4$ formation commences at 700° C in the presence of AlF_3 and the starting temperature falls by about 300° C.

Fig. 7 shows the microstructures for the system fired at 700° C. The behaviour of AlF_3 during $ZnAl_2O_4$ formation was classified into three steps from the microstructures. Fig. 7a is the microstructure in the early stage of the reaction. The reaction begins at the ZnO–AlF_3 interface and $ZnAl_2O_4$ forms in the ZnO phase close to AlF_3 particles. Alumina did not react at this stage. Therefore, the reaction occurring would be the same as that for the ZnO–AlF_3 binary system described in the preceding section. In the middle stage

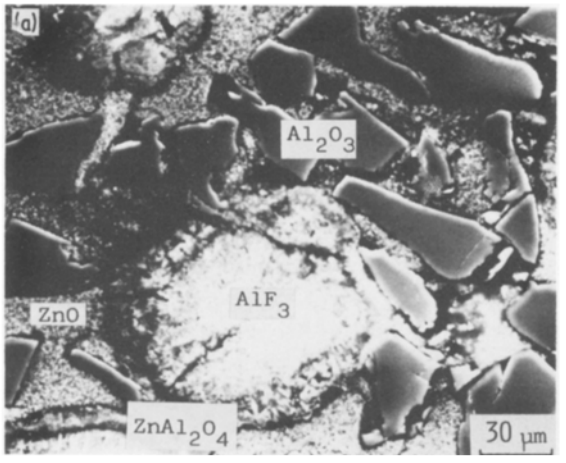

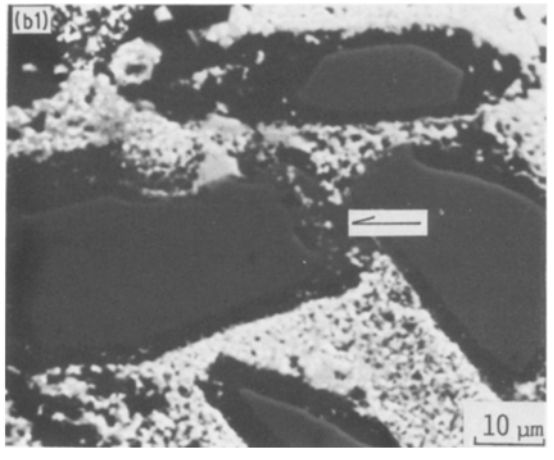

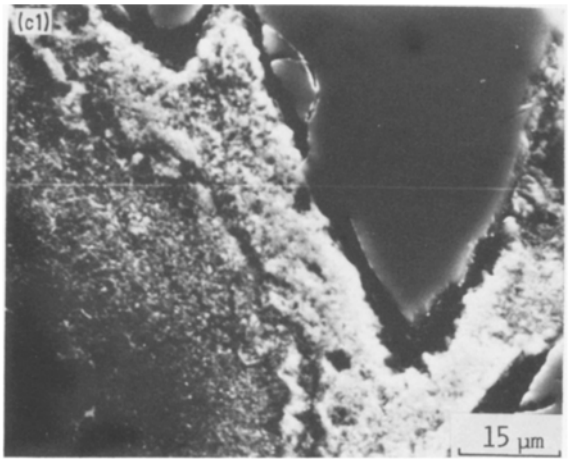

Figure 7 Microstructures for the system of ZnO, coarse Al_2O_3 and AlF_3. (a) SE image of initial stage of the reaction, (b1) SE image of middle stage of the reaction, (b2) EDX analysis of the point indicated in (b1), (c1) SE image of final stage of the reaction, (c2) X-ray line profiles of Zn*Kα* and Al*Kα* on the analysed line in (c1).

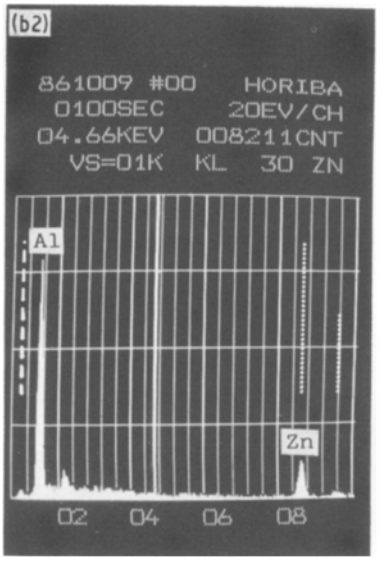

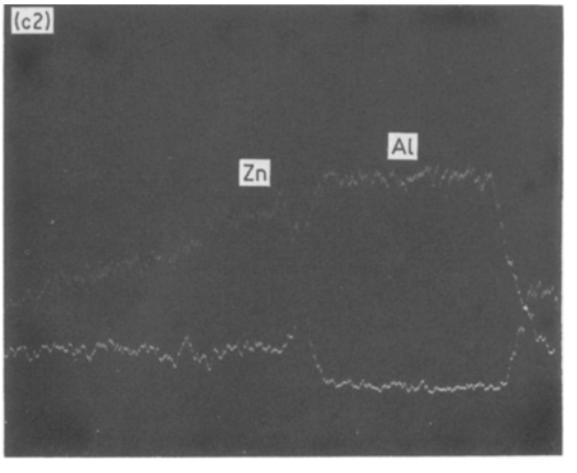

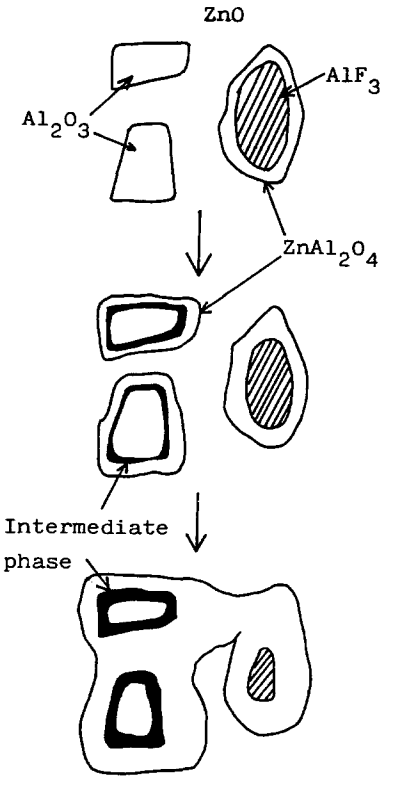

Figure 8 Schematic reaction model for the system containing coarse Al_2O_3 in the presence of AlF_3.

indicated in Fig. 7b1, a $ZnAl_2O_4$ layer develops around AlF_3 and also around Al_2O_3 particles. At this stage the Al^{3+} ion was not found in the ZnO phase. So the fluoride ion found at the Al_2O_3 interface must be carried by the Zn^{2+} ion as zinc fluoride or zinc oxyfluoride. The fluoride ion bound with zinc ion was easily transferred to the aluminium ion when the zinc oxyfluoride made contact with alumina. The edges of the alumina particles became rounded because alumina dissolved into the liquid phase, and an intermediate phase was observed around the Al_2O_3 particle. EDX analysis focusing an electron beam on the intermediate phase shows the presence of aluminium and a small amount of zinc, as indicated in Fig. 7b2. Alumina did not change in the Al_2O_3–AlF_3 binary system at this temperature, but dissolved in the ZnO–Al_2O_3–AlF_3 three-component system to form the intermediate phase and $ZnAl_2O_4$.

In the final stage of the reaction, the microstructure after firing at 700° C for 30 h is as seen in Fig. 7c1. The $ZnAl_2O_4$ layer grows into agglomerates of fine ZnO particles. Dissolution of alumina into the intermediate phase or transport process in the product layer might be the rate-controlling process of $ZnAl_2O_4$ formation at this stage. The distribution of aluminium and zinc in the product layer in Fig. 7c2, however, shows no slope. Dissolution of Al_2O_3 would, therefore, be the rate controlling process in the final stage of coarse Al_2O_3 system. Fig. 8 shows a schematic reaction model for the ZnO–coarse Al_2O_3–AlF_3 system.

3.3. $ZnAl_2O_4$ formation in ZnO–agglomerates of the fine Al_2O_3–AlF_3 system

The DTA curve for the ZnO–Al_2O_3–AlF_3 three-component system in Fig. 9 shows an exothermic

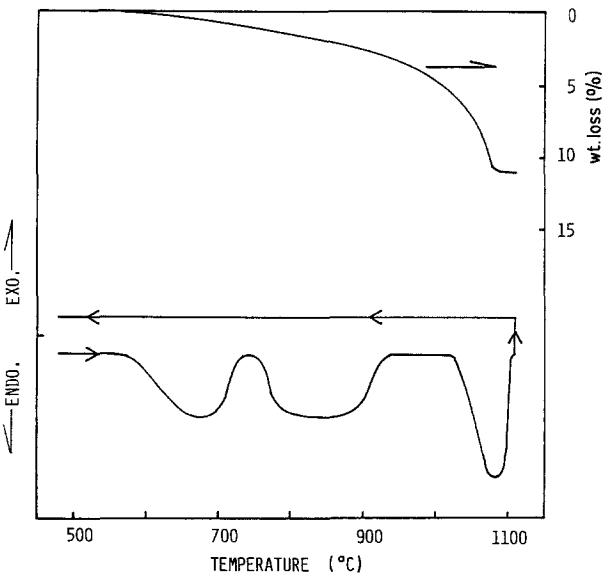

Figure 9 TG and DTA curves for ZnO, fine Al_2O_3 and AlF_3 system.

peak at 744° C on a broad endothermic peak as if the exothermic peak was superimposed on the endothermic background observed in the ZnO–AlF_3 binary system. Acidic aluminium fluoride solution which dissolved basic zinc oxide could attack aluminium oxide to form the intermediate phase leading to $ZnAl_2O_4$ formation. The microstructure of ZnO–agglomerates of the fine alumina–AlF_3 system was observed and compared with that of the coarse Al_2O_3 system.

The microstructure of the system of agglomerates of fine Al_2O_3 fired at 700° C is shown in Fig. 10. The behaviour of AlF_3 in the fine Al_2O_3 system was observed in three steps as shown in the figure. In the early stage, as shown in Fig. 10a, the reaction initiates at the ZnO–AlF_3 interface and forms $ZnAl_2O_4$, similar to the first stage for the coarse alumina system. There is, however, an apparent difference between the microstructures of the middle step for two systems as shown in Figs 10b1 and 7b where Al_2O_3 joins in the reaction to form $ZnAl_2O_4$. Zinc aluminate phase develops into agglomerates of fine Al_2O_3 particles in Fig. 10b1 in contrast to the case of the coarse Al_2O_3 system in Fig. 7b. Aluminium fluoride carries ZnO to the interspace between the fine Al_2O_3 particles in the agglomerates and then $ZnAl_2O_4$ forms. The presence of a slope of the distribution of zinc and aluminium in the product layer in Fig. 10b2 indicates that the diffusion of these cations in the product layer is the slowest step at this stage.

In the final stage, shown in Fig. 10c, ZnO agglomerates gradually dissolve into the intermediate phase and are absorbed into Al_2O_3 or AlF_3 agglomerates and disappear, leaving voids after long firing times.

4. Conclusions

1. In the ZnO–AlF_3 binary system, sublimation of AlF_3 and successive reaction with ZnO were the first routes to $ZnAl_2O_4$ formation.

2. In the ZnO–Al_2O_3–AlF_3 three component system, $ZnAl_2O_4$ formation was initiated at ZnO–AlF_3 interfaces as well as that of the ZnO–AlF_3 binary system. This reaction was used to predict the formation of unstable zinc fluoride or zinc oxyfluoride.

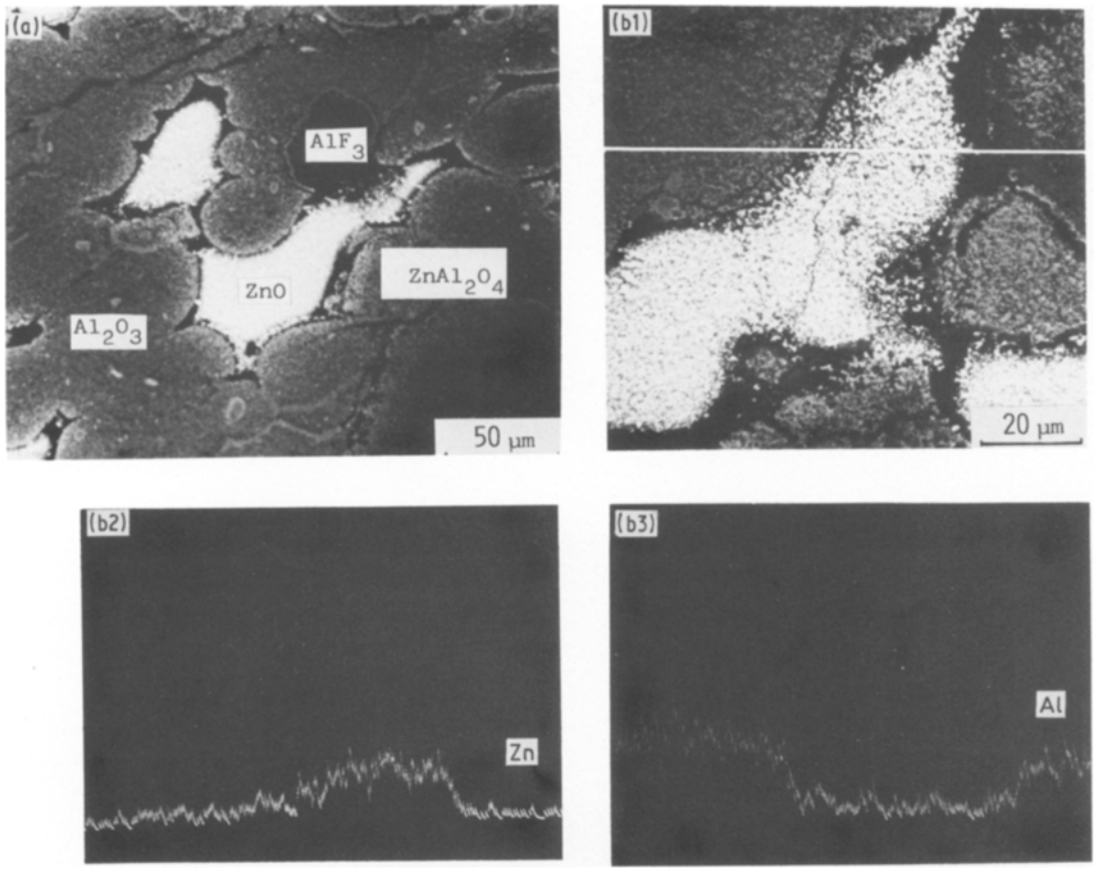

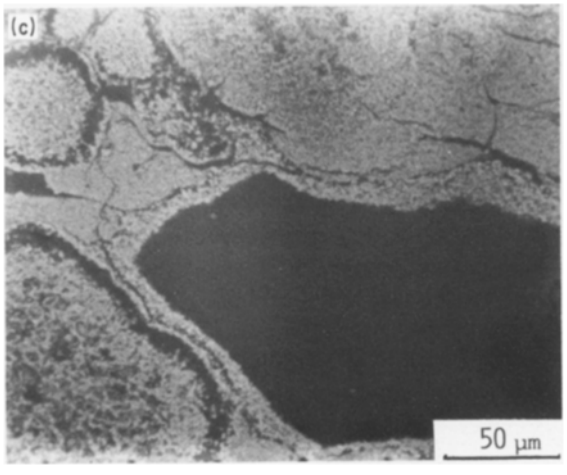

Figure 10 Microstructures for the system of ZnO, fine Al_2O_3 and AlF_3. (a) SE image of initial stage of the reaction, (b1) SE image of middle stage of the reaction, (b2) line scan of Zn$K\alpha$ on the line indicated in (b1), (b3) line scan of Al$K\alpha$ on the line indicated in (b1), (c) SE image of final stage of the reaction.

3. When the fluoride anions bound with zinc cations were transported to the surface of the Al_2O_3 particle, an intermediate phase, such as $Zn_aAl_bO_xF_y$, was formed at the site.

4. The vapour transport of AlF_3 to the ZnO–Al_2O_3 interface was expected to form the intermediate phase.

5. The $ZnAl_2O_4$ formation was promoted by the material transport through the intermediate phase around Al_2O_3 particles.

6. Coarse Al_2O_3 particles decrease the reaction rate of dissolution into the intermediate phase. On the other hand, the use of fine-particle agglomerates as starting materials changed the rate-determining step from dissolution of Al_2O_3 to the transport process in the product layer, in comparison to the coarse Al_2O_3 system.

References

1. Y. MITARAI, S. SHIRASAKI, K. MANABE and T. KUBO, *Kogyo Kagaku Zasshi* **72** (1969) 1067.
2. J. LEMAITRE and B. DELMON, *Bull. Amer. Ceram. Soc.* **59** (1980) 234.
3. Y. HAYASHI, Y. INOUE, Y. NURISHI and T. HIBINO, *Nippon Kagaku Zasshi* **92** (1971) 1119.
4. M. IGETA, K. AZUMA, Y. NURISHI and T. HIBINO, *ibid.* **92** (1971) 1126.
5. Y. ICHIKAWA, T. MURASE, Y. NURISHI and T. HIBINO, *ibid.* **92** (1971) 843.
6. S. YAMAMOTO, K. YOSHIMURA, Y. NURISHI and T. HIBINO, *Nippon Kagaku Kaishi* **93** (1972) 556.
7. M. MIYAMOTO, M. HASHIBA, Y. NURISHI and T. HIBINO, *Yogyo Kyokai-Shi* **83** (1975) 341.
8. K. YOSHIDA, M. HASHIBA, E. MIURA, Y. NURISHI and T. HIBINO, *ibid.* **84** (1976) 86.
9. E. MIURA, R. FURUMI, M. HASHIBA, Y. NURISHI and T. HIBINO, *ibid.* **88** (1980) 577.
10. R. A. EPPLER, *J. Amer. Ceram. Soc.* **62** (1979) 47.
11. *Idem, ibid.* **53** (1970) 457.
12. *Idem, Ind. Eng. Chem. Prod. Res. Develop.* **10** (1971) 352.
13. H. YANAGIDA and M. ATSUMI, *Yogyo Kyokai-Shi* **75** (1967) 349.
14. S. SHIMADA and T. ISHII, *Nippon Kagaku Kaishi* **93** (1972) 1234.
15. S. SHIMADA, R. FURUICHI and T. ISHII, *Bull. Chem. Soc. Jpn* **49** (1976) 1289.
16. T. TSUCHIDA, R. FURUICHI and T. ISHII, *Chem. Lett.* (1975) 1191.
17. S. SHIMADA, R. FURUICHI and T. ISHII, *Bull. Chem. Soc. Jpn* **47** (1974) 2026.
18. *Idem, ibid.* **47** (1974) 2031.

19. M. HASHIBA, E. MIURA, Y. NURISHI and T. HIBINO, *Nippon Kagaku Kaishi* **1983** (1983) 501.
20. M. HASHIBA and Y. NURISHI, unpublished data.
21. J. I. GOLDSTEIN, D. E. NEWBURY, P. ECHLIN, D. C. JOY, C. FIORI and E. LIFSHIN, "Scanning Electron Microscopy and X-ray Microanalysis" (Plenum, New York, 1981) p. 263.
22. IUPAC Chemical Data Series, No. 21, "Stability Constants of Metal-Ion Complexes, Part A: Inorganic Ligands", Compiled by E. Hoegfeldt (Pergamon, 1982) p. 181.
23. T. YOKOKAWA, *Tetsu to Hagane* **68** (1982) 26.
24. O. KUBASCHEWSKI, E. LL. EVANS and C. B. ALCOCK, "Metallurgical Thermochemistry", 4th Edn (Pergamon, 1967) p. 304.
25. JANAF Thermochemical Tables, 2nd Edn (Dow Chemical Co., 1970 and 1974, 1975 Supplements).
26. I. BARIN and O. KNACKE, "Thermochemical Properties of Inorganic Substances" (Springer-Verlag, 1973).

Received 23 March
and accepted 8 June 1987